Journal of Hazardous Materials 179 (2010) 438–443

Contents lists available at ScienceDirect

Journal of Hazardous Materials

journal homepage: www.elsevier.com/locate/jhazmat

Microwave-assisted preparation, characterization and photocatalytic properties of a dumbbell-shaped ZnO photocatalyst

Li-Yun Yang[a,b], Shu-Ying Dong[a], Jian-Hui Sun[a,*], Jing-Lan Feng[a], Qiu-Hua Wu[a], Sheng-Peng Sun[c,**]

[a] Henan Key Laboratory for Environmental Pollution Control, College of Chemistry and Environmental Sciences, Henan Normal University, Xinxiang, Henan 453007, PR China
[b] College of Chemistry and Chemical Engineering, Xinxiang University, Henan 453007, PR China
[c] State Key Laboratory of Pollution Control and Resources Reuse, College of Environmental Science and Engineering, Tongji University, Shanghai 200092, PR China

ARTICLE INFO

Article history:
Received 4 December 2009
Received in revised form 21 February 2010
Accepted 6 March 2010
Available online 12 March 2010

Keywords:
Dumbbell-shaped ZnO
Microwave heating
Methylene Blue
Photocatalytic
Kinetics
Langmuir–Hinshelwood model

ABSTRACT

A novel dumbbell-shaped ZnO photocatalyst was successfully synthesized by microwave heating in the present study. The prepared ZnO photocatalysts were characterized by X-ray diffraction (XRD), scanning electron microscopy (SEM) and UV–Vis absorption spectrum (UV–Vis). The results indicated that the prepared ZnO photocatalyst shows a united dumbbell shape with 2 μm diameter and 5 μm length. The photocatalytic activity of the prepared dumbbell-shaped ZnO photocatalyst was evaluated by the degradation of Methylene Blue (MB) in aqueous solution. The effects of pH, catalyst dosage ([ZnO]) and initial concentration of MB ([MB]) on the photocatalytic degradation efficiency of MB were investigated. An optimum condition was determined as pH 7–8, [ZnO] = 1.0 g-ZnO L^{-1} and [MB] = 15 mg-MB L^{-1}. Under the optimum condition, the decolorization and TOC removal efficiencies of MB at 75 min reaction time were achieved 99.6% and 74.3%, respectively, which were higher than that by the commercial ZnO powder. In addition, the photocatalytic degradation kinetics of MB was also investigated. The results showed that the photocatalytic degradation kinetics of MB fitted the pseudo-first-order kinetics and the Langmuir–Hinshelwood model.

1. Introduction

Dyes widely used in textiles, paper, rubber and plastics industries have led to severe environmental contamination due to the emitting of the toxic and colored wastewater into water bodies [1–3]. They seriously affect the nature of water, inhibit sunlight penetration and reduce photosynthetic reaction. In addition, some dyes are either toxic or carcinogenic [4,5]. The traditional techniques for the treatment of dye waste effluents are usually non-destructive, inefficient and costly or just transfer pollutions from water to another phase [2,6–8].

Recent studies have shown that heterogeneous semiconductor (TiO_2 and ZnO) photocatalysis can be an alternative to conventional methods for the removal of dye pollutants from water [9–12]. When these semiconductors are illuminated with an appropriate light source, the electron/hole pairs are produced with electrons promoted to the conduction band and leaving the positive holes in the valence band. The generated electron/hole pairs induce a complex series of reactions that might result in the complete degradation of the dye pollutants adsorbed on the semiconductor surface [9–12]. It is well known that TiO_2 is the most commonly used photocatalyst for the degradation of a wide range of organic pollutants. At the same time, ZnO as a potential photocatalyst has been also widely investigated in recent years. The biggest advantage of ZnO compared with TiO_2 is that it absorbs over a larger fraction of the UV spectrum and absorbs more light quanta than TiO_2 [13,14]. Additional, ZnO is with a lower cost and it has shown higher photocatalytic efficiencies for the degradation of several organic pollutants in both acidic and basic medium than TiO_2 [15,16].

It has been demonstrated that the structural and morphological characters such as the size, shape, crystalline form, photocatalytic activity and some relevant properties of ZnO can be significantly affected by different synthesis methods [17–19]. Up to now, various methods have been developed to prepare ZnO photocatalyst with special performance, which mainly include hydrolysis in polyol medium [20], template method [21], chemical-precipitation [22], thermal oxidation process [18], hydrothermal synthesis [23] and microwave heating [24]. Among these methods, microwave heating is a simple fast and safe synthesis method which entirely differs from other synthesis techniques [25].

Dumbbell shaped ZnO has received some attention due to its excellent gas sensing and optical properties [26,27]. It has been synthesized by hydrothermal, wet chemical and solution methods, however, these methods were complex or relative time-consuming [28–30]. Therefore, the aim of the present study was to investigate the synthesis of a dumbbell-shaped ZnO photocatalyst via

* Corresponding author. Tel.: +86 373 3325971; fax: +86 373 3326336.
** Corresponding author. Tel.: +86 21 6598 2692; fax: +86 21 6598 2689.
E-mail addresses: sunsp_hj@yahoo.com.cn (J.-H. Sun), sunsp@yahoo.cn (S.-P. Sun).

0304-3894/$ – see front matter © 2010 Elsevier B.V. All rights reserved.
doi:10.1016/j.jhazmat.2010.03.023

microwave heating and without the addition of any surfactant. The morphology, microstructure and optical properties of the prepared ZnO photocatalyst were characterized by X-ray diffraction (XRD), scanning electron microscopy (SEM) and UV–Vis absorption spectrum (UV–Vis). The photocatalytic activity of the prepared ZnO photocatalyst was evaluated by the degradation of Methylene Blue (MB) under UV light irradiation. The characterizations and photocatalytic activity of dumbbell-shaped ZnO were compared with the commercial ZnO. The effect of various operating parameters such as pH, catalyst dosage and the initial dye concentration on the degradation of MB were investigated. In addition, the degradation kinetics of MB was also studied.

2. Materials and methods

2.1. Materials

Zinc acetate dihydrate ($Zn(CH_3COO)_2{\cdot}2H_2O$) and commercial ZnO powder were purchased from Tianjin Chemical Reagent Factory (Tianjin, China). Ammonia solution (NH_4OH), Methylene Blue, Hydrochloric acid (HCl) and Sodium hydroxide (NaOH) were purchased from Shanghai Chemical Reagent Company (Shanghai, China). All chemicals used in this study were analytical grade and used directly without further purification. Deionized water with conductivity between 0.7 and 1.0 $\mu S\,cm^{-1}$ was used throughout this study.

2.2. Dumbbell-shaped ZnO photocatalyst preparation

5 g $Zn(CH_3COO)_2{\cdot}2H_2O$ was dissolved in 30 mL deionized water, 8 mL NH_4OH was dropwise added to the above solution under magnetic stirring. After 10 min of stirring, the reaction mixture was poured into a PTFE sealed can and heated in a microwave oven (Midea KD21B-C, 2.45 GHz, Shunde Medea Microwave Oven Production Co. Ltd., Foshan, China) at a power of 400 W for 5 min, followed by 240 W for 10 min. After that the PTFE sealed can was cooled down to room temperature, the colloid material was filtered and washed with deionized water in order to remove undesirable anions such as CH_3COO^-, dried at 80 °C for 5 h and then calcined at 500 °C with air atmosphere in an oven for 1 h. After cooling down to room temperature, the dumbbell-shaped ZnO photocatalyst was obtained.

2.3. Dumbbell-shaped ZnO photocatalyst characterization

The crystal structure of the prepared ZnO microcrystal photocatalyst was analyzed by XRD. The patterns were recorded in the 2θ range of 10–70° with a scan rate of 0.02°/0.4 s by using a Bruker-D8-AXS diffractometer system equipped with a Cu Kα radiation (λ = 0.15406 Å) (Bruker Co., Germany). The morphology and dimensions of ZnO microcrystal photocatalyst were observed by SEM (JSM-6301, Japan). The UV–Vis spectra of ZnO microcrystal photocatalyst were measured by using a UV–Vis spectrophotometer (Lambda 17, Perkin-Elmer), prior to UV–Vis analysis the ZnO sample was ultrasonically dispersed in deionized water at room temperature.

2.4. Photocatalytic experiments

The photocatalytic activity of the prepared ZnO microcrystal photocatalyst was evaluated by the degradation of MB dye wastewater. All experiments were carried out in a photo-reaction apparatus as reported in our previous studies [31]. A 300 W high-pressure mercury lamp with the strongest emission at 365 nm was used as light source (Yaming Company, Shanghai). Prior to each test, the lamp was turned on and warm up for about 10 min in order to get a constant output. Batch tests were performed as the following procedure, 1 g ZnO photocatalyst was added into 1000 mL dyes solutions, the mixture was stirred in dark for 40 min to allow the physical adsorption of dyes molecules on catalyst particles reaching the equilibrium. Subsequently, the mixture was poured into the photoreactor and began the photocatalytic degradation tests. The reaction solution was mixed by an air diffuser, which was placed at the bottom of the reactor to uniformly disperse air into the solution with a flow rate of 0.2 $m^3\,h^{-1}$. The temperature of the reactions was controlled at room temperature by circulating water. The pH of dyes wastewater was adjusted to the required pH by adding 0.1 M HCl or NaOH. The pH value of solutions was measured by a pHS-3C digital pH meter. The photocatalytic activity of the prepared ZnO photocatalyst was compared with the commercial ZnO under the same conditions.

Samples were collected at regular intervals and were immediately centrifuged to remove particles for analysis. The concentration of MB was determined by measuring the absorption intensity at its maximum absorbance wavelength of λ_{MB} = 661 nm, by using a UV–Vis spectrophotometer (Lambda 17, Perkin-Elmer) with a 1 cm path length spectrometric quartz cell, and then calculated from calibration curve. The TOC of the samples were analyzed by using a TOC analyzer (Apollo 9000, Terkmar-Dohrmann, USA). The degradation of the dyes wastewater was defined as follows:

$$\eta = \frac{C_0 - C_t}{C_0} \times 100\% \quad (1)$$

where η is the decolorization efficiency or TOC removal efficiency of the dye wastewater, C_0 is the initial dye concentration or TOC concentration, C_t is the dye concentration or TOC concentration at certain reaction time t (min).

3. Results and discussion

3.1. Characterizations

The XRD spectra of the prepared ZnO photocatalyst and commercial ZnO are shown in Fig. 1. A series of characteristic peaks are observed, 2.8143 (1 0 0), 2.6033 (0 0 2), 2.4759 (1 0 1), 1.9111 (1 0 2), 1.6247 (1 1 0), 1.4771(1 0 3), 1.4072 (2 0 0), 1.3782 (1 1 2) and 1.3583 (2 0 1) which were in accordance with the hexagonal wurtzite structure of ZnO (International Center for Diffraction Data, JCPDS 36-1541). No any other impure diffraction peaks were detected, indicating that the prepared ZnO photocatalyst were pure.

SEM images of the prepared ZnO photocatalyst are shown in Fig. 2(a)–(c). It can be seen that the prepared ZnO photocatalyst show a united dumbbell shape (Fig. 2(a)). The mean diameter and length were determined at about 2 and 5 μm, respectively. In addition, from the magnification images of the dumbbell-shaped

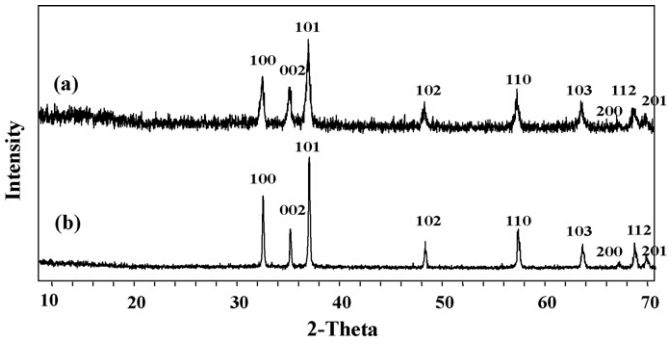

Fig. 1. The XRD patterns of the prepared ZnO photocatalyst (a) and commercial ZnO (b).

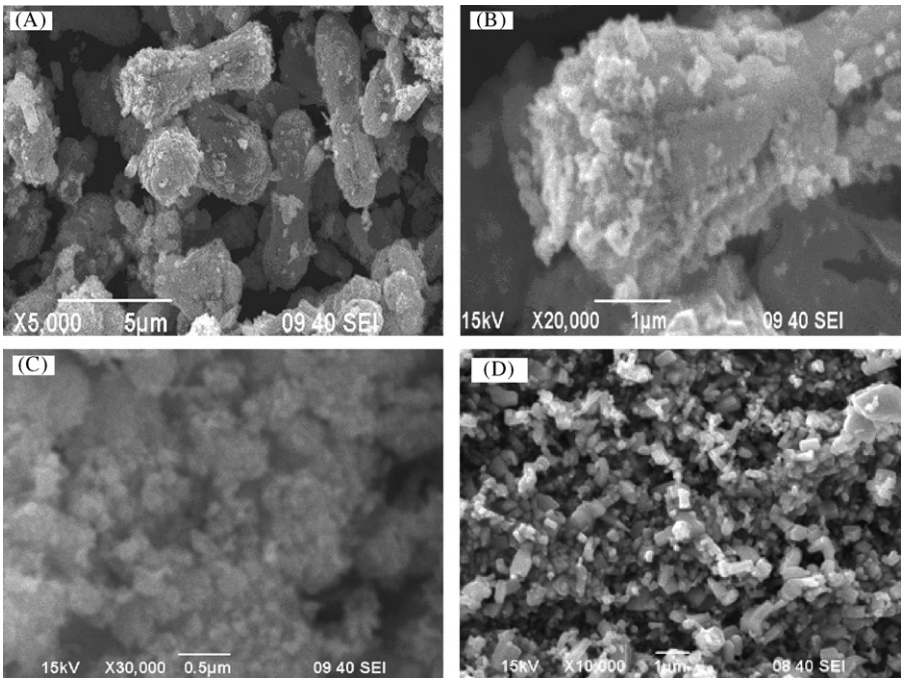

Fig. 2. SEM images of the dumbbell-shaped ZnO photocatalyst (a, b and c) and commercial ZnO (d).

ZnO (Fig. 2(b) and (c)), it can be observed that the surface of the prepared ZnO photocatalyst was covered by a lot of small particles (the particles size was about 100 nm). These small particles might increase the surface area of the prepared ZnO photocatalyst and enhance its light absorption, which might be beneficial for its photocatalytic activity enhancement. In addition, although various microstructures and small diameter of particles was observed for the commercial ZnO (Fig. 2(d)), it seems like the commercial ZnO particles are easily agglomerate between each other, which might result in decreasing the light utilization rate and lower its photocatalytic activity.

It is well known that the optical absorption behavior of photocatalyst could significantly affect its photocatalytic activity. Fig. 3 shows the UV–Vis absorption spectra of the prepared dumbbell-shaped ZnO photocatalyst and commercial ZnO. An absorption peak centered at 358 nm was found from the spectra of the prepared dumbbell-shaped ZnO photocatalyst. It can be seen that the absorbance of the prepared dumbbell-shaped ZnO photocatalyst was quickly increased as decreasing the wavelength from 500 to 358 nm. However, the absorbance of commercial ZnO was slightly increased as decreasing the wavelength within the same region. In addition, it was also observed that the absorbance of the prepared dumbbell-shaped ZnO photocatalyst was higher than commercial ZnO at the whole UV region from 200 to 358 nm. The results indicated that the prepared dumbbell-shaped ZnO photocatalyst showed good optical absorption behavior, especially for UV light absorption.

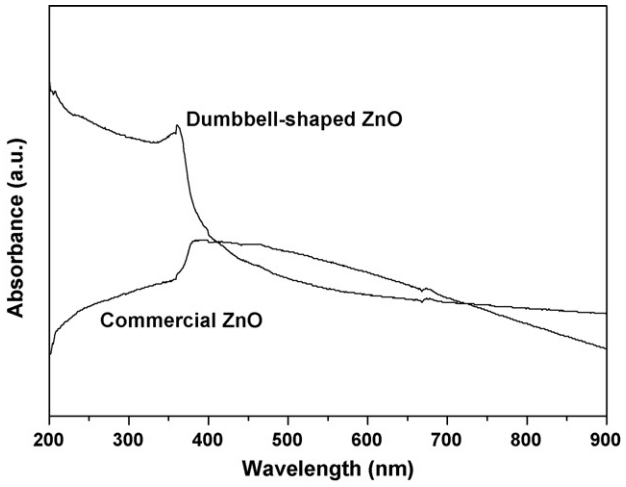

Fig. 3. UV–Vis absorption spectra of the dumbbell-shaped ZnO photocatalyst and commercial ZnO at room temperature.

3.2. Photocatalytic activity of the dumbbell-shaped ZnO photocatalyst

3.2.1. Effect of pH

The effect of pH on the photocatalytic activity of the dumbbell-shaped ZnO photocatalyst was tested and the results are shown in Fig. 4. It can be seen that pH can significantly affect the photocatalytic activity of the dumbbell-shaped ZnO photocatalysts, an optimal pH was found to be 6.9–7.8. As shown in Fig. 4, the decolorization efficiency of MB was significantly increased from 25.8% to 99.6% with increasing pH from 5.6 to 6.9. However, the decolorization efficiency was gradually decreased with further increasing pH above 7.8. The pH effect on the photocatalytic activity of the dumbbell-shaped ZnO photocatalyst can be explained on the basis of the point of zero charge of ZnO. Changes of pH shift the redox-potentials of valence and conduction bands, which might affect the interfacial charge-transfer [32,33]. At a low pH, the surface of ZnO photocatalyst is positively charged, but at a high pH it becomes negatively charged. Since MB is a cationic dye, high pH favors the adsorption of MB molecule on the catalyst surface which results in a high decolorization efficiency of MB under neutral and basic conditions. However, the stability of ZnO might not be guaranteed at high pH due to the possibility of alkaline dissolution of ZnO [34,35].

3.2.2. Effect of the catalyst dosage

The effect of catalyst dosage on the photocatalytic degradation of MB was tested and the results are shown in Fig. 5. It can be

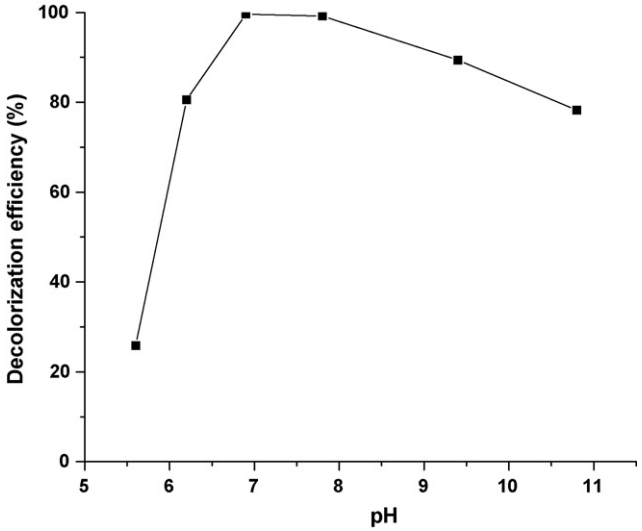

Fig. 4. Effect of pH on the photocatalytic activity of the dumbbell-shaped ZnO photocatalyst. Experimental conditions: [dye] = 15 mg L^{-1}, [ZnO] = 1.0 g L^{-1}, gas flow rate = 0.2 m^3 h^{-1}, temperature = 22 °C and reaction time = 75 min.

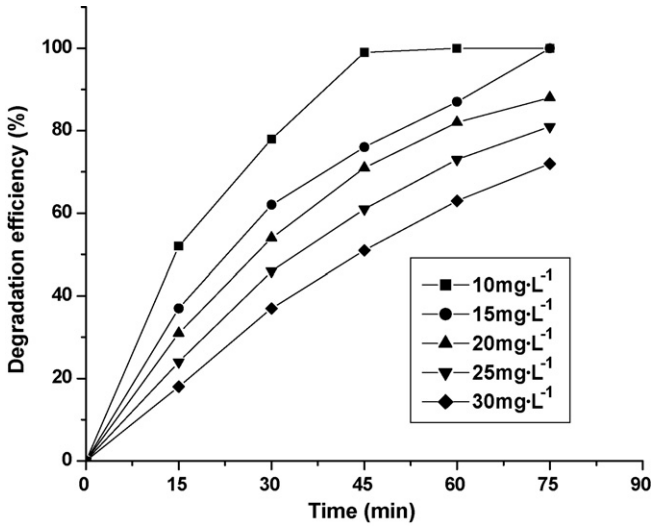

Fig. 6. Effect of initial dye concentration on the photocatalytic degradation of MB by the dumbbell-shaped ZnO photocatalyst. Experimental conditions: pH 6.9, [ZnO] = 1.0 g L^{-1}, gas flow rate = 0.2 m^3 h^{-1} and temperature = 22 °C.

seen that the decolorization efficiency of MB increased from 76% to 99.6% with increasing the dosage of ZnO photocatalyst from 0.5 to 1.0 g L^{-1}. This is due to with the increase of the catalyst dosage, the photogenerated electron hole pairs and •OH were correspondingly increased, which lead to more dye molecules destruction. However, it does not mean that the more catalyst dosage, the higher degradation efficiency of MB. We can clearly observe that when increasing the dosage of ZnO photocatalyst from 1.0 to 2.5 g L^{-1}, the decolorization efficiency of MB was decreased by 22.6% but not increased. It can be explained by the fact that when the catalyst dosage was bigger than a certain value, too much catalyst could cripple the solution's transparence and cause a scattering effect, correspondingly reduce the light utilization rate and lower the photocatalytic activity of ZnO. Therefore, the results show that an optical dosage of ZnO photocatalyst for the degradation of MB is 1.0 g L^{-1}.

3.2.3. Effect of initial concentration of MB

The effect of initial concentration of MB on the photocatalytic degradation efficiency was tested by varying the initial concentration of MB from 10 to 30 mg L^{-1}, the results are shown in Fig. 6. It was found that the decolorization efficiency of MB was strongly depended on the initial dye concentration. The decolorization efficiency of MB was decreased from 100% to 72% with the increase of the initial dye concentration from 10 to 30 mg L^{-1}. An explanation was that as the initial concentration of MB was increased, the dosage of generated •OH was not correspondingly increased due to the same dosage of ZnO photocatalyst, which resulted in a relative small •OH concentration. In addition, high concentration of dye might also decrease the light utilization rate by ZnO photocatalyst, thus the photodegradation efficiency of MB was decreased with the increase of the initial dye concentration [36].

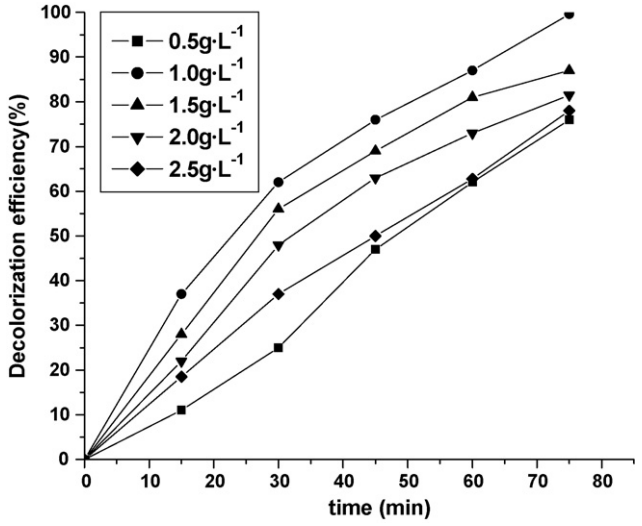

Fig. 5. Effect of catalyst dosage on the photocatalytic degradation of MB by the dumbbell-shaped ZnO photocatalyst. Experimental conditions: [dye] = 15 mg L^{-1}, pH 6.9, gas flow rate = 0.2 m^3 h^{-1} and temperature = 22 °C.

3.2.4. Comparison of the photocatalytic activity of the dumbbell-shaped ZnO and commercial ZnO

Fig. 7 shows the comparison of the decolorization and TOC removal efficiencies of MB in aqueous solution by dumbbell-shaped ZnO photocatalyst and commercial ZnO. It can be seen that the decolorization efficiency and TOC removal efficiency of MB by the dumbbell-shaped ZnO photocatalyst after 75 min reaction time was achieved 99.6% and 74.3%, respectively, which was 6.9% and 19.8%

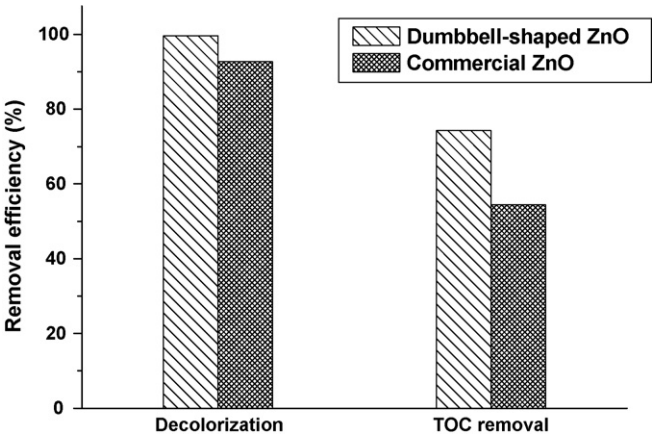

Fig. 7. Decolorization and TOC removal efficiencies of MB by the dumbbell-shaped ZnO photocatalyst and commercial ZnO. Experimental conditions: [dye] = 15 mg L^{-1}, pH 6.9, [ZnO] = 1.0 g L^{-1}, gas flow rate = 0.2 m^3 h^{-1}, temperature = 22 °C and reaction time = 75 min.

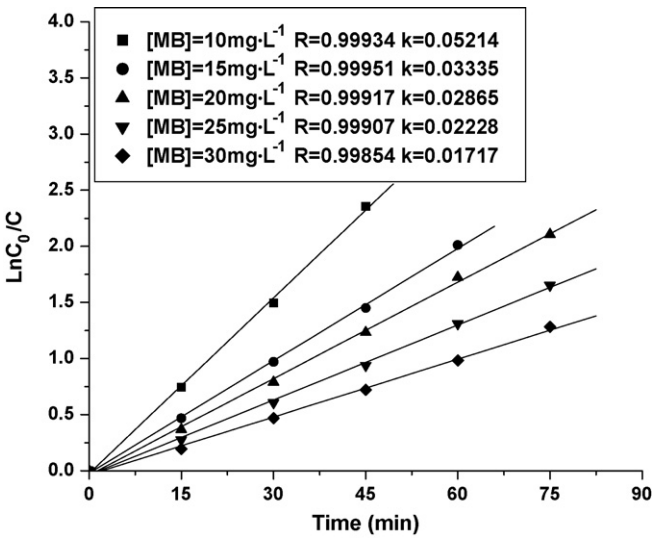

Fig. 8. The plots of $\ln C_0/C$ versus reaction time (t, min) with different initial concentrations of MB. Experimental conditions: [dye] = 15 mg L^{-1}, pH 6.9, [ZnO] = 1.0 g L^{-1}, gas flow rate = 0.2 m^3 h^{-1} and temperature = 22 °C.

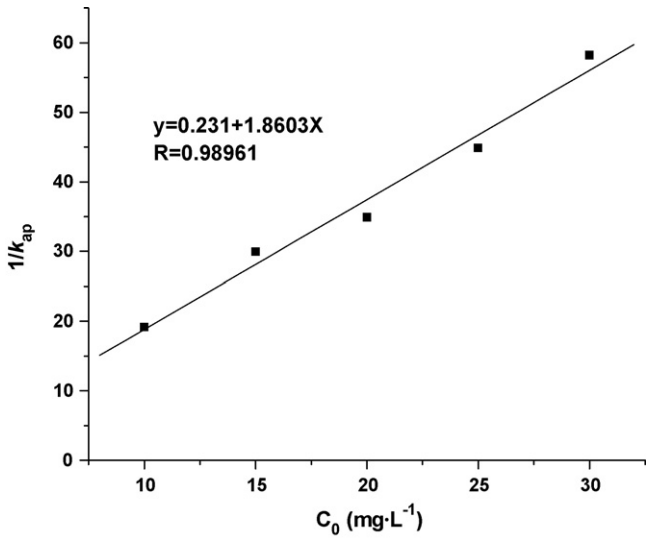

Fig. 9. The relationship between the $1/k_{ap}$ and the initial concentration of MB. Experimental conditions: [dye] = 15 mg L^{-1}, pH 6.9, [ZnO] = 1.0 g L^{-1}, gas flow rate = 0.2 m^3 h^{-1}, temperature = 22 °C and reaction time = 75 min.

higher than that by the commercial ZnO. In addition, Jang et al. [37] reported that the maximum photocatalytic decolorization efficiencies of 10–20 mg L^{-1} MB by 1.0 g L^{-1} ZnO nanoparticles and ZnO nano-crystalline particles after 120 min reaction time were achieved 99–97% and 93–77%, respectively. Kim and Park [38] reported that the maximum photocatalytic decolorization efficiencies of 6 mg L^{-1} MB by 1.5 g L^{-1} rod- and spherical-shaped ZnO nanoparticles after 100 min reaction time were achieved 75% and 98.5%, respectively. Chakrabarti and Dutta [33] reported that the maximum photocatalytic decolorization efficiencies of 25 mg L^{-1} MB by 1.0 g L^{-1} GR grade commercial ZnO after 120 min reaction time achieved 93%. Height et al. [39] reported that the maximum photocatalytic decolorization efficiencies of 10 mg L^{-1} MB by 0.3 g L^{-1} flame-made Ag-ZnO (Ag loading was 3 at.%) after 60 min reaction time achieved 54%. The results above indicate that the prepared dumbbell-shaped ZnO photocatalyst shows a good photocatalytic activity, which might be attributed to its unique microstructure to absorb a large fraction of UV light. On the contrary, the agglomerate of commercial ZnO particles decreased the UV light utilization rate, which reduced its photocatalytic activity and resulted in a low decolorization efficiency of MB.

3.3. Kinetics analysis

In the present study, it was found that the photocatalytic degradation of MB by the dumbbell-shaped ZnO photocatalyst was obeyed the pseudo-first-order kinetics. The pseudo-first-order kinetics for MB's degradation was calculated as follows (Eq. (2) and Eq. (3)):

$$-\frac{dC}{dt} = kC \tag{2}$$

$$\ln\left(\frac{C_0}{C}\right) = kt \tag{3}$$

where k is the pseudo-first-order rate constant (min^{-1}), C_0 is the initial concentration of MB (mg L^{-1}), C is the concentration of MB at reaction time t (min). The linear plots of $\ln(C_0/C)$ versus irradiation time t (min) are shown in Fig. 8. It can be seen that the relationship between $\ln(C_0/C)$ and irradiation time t was in a good linear ($R > 0.99$).

In principle, the photocatalytic degradation of MB by the dumbbell-shaped ZnO photocatalyst is an interface process, which might follow the Langmuir–Hinshelwood model (Eq. (4) and Eq. (5)):

$$r_0 = -\frac{dC}{dt} = \frac{K_1K_2C}{1+K_2C_0} = k_{ap}C \tag{4}$$

$$\frac{1}{k_{ap}} = \frac{1}{K_1K_2} + \frac{C_0}{K_1} \tag{5}$$

where C_0 is the initial concentration of MB (mg L^{-1}), K_1 is the surface reaction rate constant (mg L^{-1} min^{-1}), K_2 is the Langmuir–Hinshelwood adsorption equilibrium constant (L mg^{-1}) and k_{ap} (min^{-1}) is the pseudo-first-order rate constant. A plot of $1/k_{ap}$ versus C_0 for the photocatalytic degradation of MB is shown in Fig. 9. A linear relation between the $1/k_{ap}$ and dye concentration was observed ($R = 0.98961$), which indicated that the photocatalytic degradation of MB by dumbbell-shaped ZnO photocatalyst followed the Langmuir–Hinshelwood model. The surface reaction rate constant and the adsorption equilibrium constant were calculated as $K_1 = 0.5375$ mg L^{-1} min^{-1} and $K_2 = 8.054$ L mg^{-1}, respectively. The results were consistent with the other reports [33–35].

4. Conclusions

In this study, a dumbbell-shaped ZnO photocatalyst was successfully synthesized via microwave-heating method. The prepared dumbbell-shaped ZnO photocatalyst were characterized by XRD, SEM and UV–Vis absorption spectra. The photocatalytic activity of the prepared dumbbell-shaped ZnO photocatalyst was evaluated by the degradation of MB in aqueous solution. The results indicated that pH can significantly affect the photocatalytic activity of the dumbbell-shaped ZnO photocatalysts, an optimal pH was found to be 6.9–7.8. In addition, an optical catalyst dosage and dye concentration was found to be 1.0 g-ZnO L^{-1} and 15 mg-MB L^{-1}. Under the optical conditions, the decolorization efficiency and TOC removal efficiency at 75 min reaction time were achieved 99.6% and 74.3%, respectively, which was higher than that by the commercial ZnO powder. Moreover, it was found that the degradation kinetics of MB fitted the pseudo-first-order kinetics and the Langmuir–Hinshelwood model. The surface reaction rate constant and the adsorption equilibrium constant was calculated as $K_1 = 0.5375$ mg L^{-1} min^{-1} and $K_2 = 8.054$ L mg^{-1}, respectively.

Acknowledgements

This work was supported by the Natural Science Research Foundation of Henan province, PR China (Grant No. 0611020900 and No. 102300410098). The authors also would like to thank Shanghai Tongji Gao Tingyao Environmental Science & Technology Development Foundation (STGEF).

References

[1] A. Houas, H. Lachheb, M. Ksibi, E. Elaloui, C. Guillard, J.M. Herrmann, Photocatalytic degradation pathway of methylene blue in water, Appl. Catal. B: Environ. 31 (2001) 145–157.
[2] I.K. Konstantinou, T.A. Albanis, TiO_2-assisted photocatalytic degradation of azo dyes in aqueous solution: kinetic and mechanistic investigations: a review, Appl. Catal. B: Environ. 49 (2004) 1–14.
[3] P.A. Pekakis, N.P. Xekoukoulotakis, D. Mantzavinos, Treatment of textile dyehouse wastewater by TiO_2 photocatalysis, Water Res. 40 (2006) 1276–1286.
[4] A. Criscuoli, J. Zhong, A. Figoli, M.C. Carnevale, R. Huang, E. Drioli, Treatment of dye solutions by vacuum membrane distillation, Water Res. 42 (2008) 5031–5037.
[5] M. Constapel, M. Schellentrager, J.M. Marzinkowski, S. Gäb, Degradation of reactive dyes in wastewater from the textile industry by ozone: analysis of the products by accurate masses, Water Res. 43 (2009) 733–743.
[6] V. Meshko, L. Markovska, M. Mincheva, A.E. Rodrigues, Adsorption of basic dyes on granular acivated carbon and natural zeolite, Water Res. 35 (2001) 3357–3366.
[7] S. Raghu, C.A. Basha, Chemical or electrochemical techniques, followed by ion exchange, for recycle of textile dye wastewater, J. Hazard. Mater. 149 (2007) 324–330.
[8] F. Harrelkas, A. Azizi, A. Yaacoubi, A. Benhammou, M.N. Pons, Treatment of textile dye effluents using coagulation–flocculation coupled with membrane processes or adsorption on powdered activated carbon, Desalination 235 (2009) 330–339.
[9] H. Kyung, J. Lee, W. Choi, Simultaneous and synergistic conversion of dyes and heavy metal ions in aqueous TiO_2 suspensions under visible-light illumination, Environ. Sci. Technol. 39 (2005) 2376–2382.
[10] E.R. Carraway, A.J. Hoffmann, M.R. Hoffmann, Photocatalytic oxidation of organic acids on quantum-sized semiconductor colloids, Environ. Sci. Technol. 28 (1994) 786–793.
[11] I. Poulios, D. Makri, X. Prohaska, Photocatalytic treatment of olive milling waste water oxidation of protocatechuic acid, Global Nest: Int. J. 1 (1999) 55–62.
[12] B. Pall, M. Sharan, Enhanced photocatalytic activity of highly porous ZnO thin films prepared by sol–gel process, Mater. Chem. Phys. 76 (2002) 82–87.
[13] M.L. Curri, R. Comparelli, P.D. Cozzoli, G. Mascolo, A. Agostiano, Colloidal oxide nanoparticles for the photocatalytic degradation of organic dye, Mater. Sci. Eng. C 23 (2003) 285–289.
[14] C.C. Chen, H.J. Fan, J.L. Jan, Degradation pathways and efficiencies of acid blue 1 by photocatalytic reaction with ZnO nanopowder, J. Phys. Chem. C 112 (2008) 11962–11972.
[15] J.C. Lee, S. Park, H.J. Park, J.H. Lee, H.S. Kim, Y.J. Chung, Photocatalytic degradation of TOC from aqueous phenol solution using solution combusted ZnO nanopowders, J. Electroceram. 22 (2009) 110–113.
[16] J.G. Yu, X.X. Yu, Hydrothermal synthesis and photocatalytic activity of zinc oxide hollow spheres, Environ. Sci. Technol. 42 (2008) 4902–4907.
[17] X.Y. Shi, M.W. Shen, H. Mohwald, Polyelectrolyte multilayer nanoreactors toward the synthesis of diverse nanostructured materials, Prog. Polym. Sci. 29 (2004) 987–1019.
[18] Y. Zhang, W.F. Zhang, H.W. Zheng, Fabrication and photoluminescence properties of ZnO: Zn hollow microspheres, Scripta Mater. 57 (2007) 313–316.
[19] M.S. Mohajerani, M. Mazloumi, A. Lak, A. Kajbafvala, S. Zanganeh, S.K. Sadrnezhaad, Self-assembled zinc oxide nanostructures via a rapid microwave-assisted route, J. Cryst. Growth 310 (2008) 3621–3625.
[20] L. Poul, S. Ammar, N. Jouini, F. Fieóvet, F. Villain, Metastable solid solutions in the system ZnO-CoO: synthesis by hydrolysis in polyol medium and study of the morphological characteristics, Solid State Sci. 3 (2001) 31–42.
[21] H.M. Kou, J. Wang, Y.B. Pan, J.K. Guo, Fabrication of hollow ZnO microsphere with zinc powder precursor, Mater. Chem. Phys. 99 (2006) 325–328.
[22] S.M. Wang, Z.S. Yang, M.K. Lu, Y.Y. Zhou, G.J. Zhou, Z.F. Qiu, S.F. Wang, H.P. Zhang, A.Y. Zhang, Coprecipitation synthesis of hollow Zn_2SnO_4 spheres, Mater. Lett. 61 (2007) 3005–3008.
[23] H. Zhou, T.X. Fan, D. Zhang, Hydrothermal synthesis of ZnO hollow spheres using spherobacterium as biotemplates, Microporous Mesoporous Mater. 100 (2007) 322–327.
[24] I.A. Siddiquey, T. Furusawa, M. Sato, N. Suzuki, Microwave-assisted silica coating and photocatalytic activities of ZnO nanoparticles, Mater. Res. Bull. 43 (2008) 3416–3424.
[25] S. Komarneni, M. Bruno, E. Mariani, Synthesis of ZnO with and without microwaves, Mater. Res. Bull. 35 (2000) 1843–1847.
[26] Z.G. Chen, A.Z. Ni, F. Li, H.T. Cong, H.M. Cheng, G.Q. Lu, Synthesis and photoluminescence of tetrapod ZnO nanostructures, Chem. Phys. Lett. 434 (2007) 301–305.
[27] R.H. Wang, J.H. Xin, X.M. Tao, UV-blocking property of dumbbell-shaped ZnO crystallites on cotton fabrics, Inorg. Chem. 44 (2005) 3926–3930.
[28] J.H. Sun, S.Y. Dong, Y.K. Wang, S.P. Sun, Preparation and photocatalytic property of a novel dumbbell-shaped ZnO microcrystal photocatalyst, J. Hazard. Mater. 172 (2009) 1520–1526.
[29] S.C. Navale, S.W. Gosavi, I.S. Mulla, Controlled synthesis of ZnO from nanospheres to micro-rods and its gas sensing studies, Talanta 75 (2008) 1315–1319.
[30] Q. Qi, T. Zhang, L. Liu, X.J. Zheng, Q.J. Yu, Y. Zeng, H.B. Yang, Selective acetone sensor based on dumbbell-like ZnO with rapid response and recovery, Sens. Actuators B: Chem. 134 (2008) 166–170.
[31] J.H. Sun, X.L. Wang, J.Y. Sun, R.X. Sun, S.P. Sun, L.P. Qiao, Photocatalytic degradation and kinetics of Orange G using nano-sized Sn(IV)/TiO_2/AC photocatalyst, J. Mol. Catal. A: Chem. 260 (2006) 241–246.
[32] Y.H. Jiang, Y.M. Sun, H. Liu, F.H. Zhu, H.B. Yin, Solar photocatalytic decolorization of C.I. Basic Blue 41 in an aqueous suspension of TiO_2-ZnO, Dyes Pigm. 78 (2008) 77–83.
[33] S. Chakrabarti, B.K. Dutta, Photocatalytic degradation of model textile dyes in wastewater using ZnO as semiconductor catalyst, J. Hazard. Mater. 112 (2004) 269–278.
[34] A.N. Rao, B. Sivasankar, V. Sadasivam, Kinetic study on the photocatalytic degradation of salicylic acid using ZnO catalyst, J. Hazard. Mater. 166 (2009) 1357–1361.
[35] U.I. Gaya, A.H. Abdullah, Z. Zainal, M.Z. Hussein, Photocatalytic treatment of 4-chlorophenol in aqueous ZnO suspensions: intermediates, influence of dosage and inorganic anions, J. Hazard. Mater. 168 (2009) 57–63.
[36] M.A. Behnajady, N. Modirshahla, R. Hamzavi, Kinetic study on photocatalytic degradation of C.I. Acid Yellow 23 by ZnO photocatalyst, J. Hazard. Mater. B 133 (2006) 226–232.
[37] Y.J. Jang, C. Simer, T. Ohm, Comparison of zinc oxide nanoparticles and its nano-crystalline particles on the photocatalytic degradation of methylene blue, Mater. Res. Bull. 41 (2006) 67–77.
[38] S.J. Kim, D.W. Park, Preparation of ZnO nanopowders by thermal plasma and characterization of photo-catalytic property, Appl. Surf. Sci. 255 (2009) 5363–5367.
[39] M.J. Height, S.E. Pratsinis, O. Mekasuwandumrong, Piyasan Praserthdam, Ag-ZnO catalysts for UV-photodegradation of methylene blue, Appl. Catal. B: Environ. 63 (2006) 305–312.